N91-17091

THE NAVSTAR GPS MASTER CONTROL STATION'S KALMAN FILTER EXPERIENCE

Michael P. Scardera, Captain, USAF

2d Satellite Control Squadron
Falcon AFB, CO. 80912-5000

ABSTRACT

The Navstar Global Positioning System is a highly accurate, space based navigation system providing all weather, 24 hour-a-day service to both military and civilian users. The Navstar system provides a Gaussian position solution with four satellites, each providing its ephemeris and clock offset with respect to GPS time. Currently, GPS is building towards the full 24 satellite constellation.

The GPS Master Control Station (MCS) is charged with tracking each Navstar spacecraft and precisely defining the ephemeris and clock parameters for upload into the vehicle's navigation message. This paper briefly describes the Navstar system and the Kalman Filter estimation process used by the MCS to determine, predict, and quality control each satellite's ephemeris and clock states. Routine performance is shown. Kalman Filter reaction and response is discussed for anomalous clock behavior and trajectory perturbations.

Particular attention is given to MCS efforts to improve orbital adjust modeling. The satellite out of service time due to orbital maneuvering has been reduced in the past year from four days to under twelve hours. The planning, reference trajectory model, and Kalman Filter management improvements are explained.

Finally, this paper will summarize the future work to improve Kalman Filter and orbital adjust performance. Reccomendations will be made for future systems requiring precise ephemerides.

INTRODUCTION

The Navstar Global Positioning System (GPS) is a satellite based radionavigation system providing worldwide all weather coverage to both civilian and military users. The Navstar system promises a revolution in all activities requiring precise navigation or positioning. GPS signals will provide the precise positioning service to authorized users of 16 meters spherical error probable (SEP) and 100 meter circular error probable (CEP) to standard positioning service customers. The standard positioning service is subject to change according to United States national interests. GPS is made up of three segments. The space segment consists of the orbiting satellites and provides L-Band signals with modulated data to the world. The User segment represents the customers who receive and utilize the navigation data. Finally, the control segment comprises a system of L-Band monitor stations, S-band ground antennas, and a control center to monitor the satellites health and periodically upload new navigation parameters. GPS is currently the largest satellite constellation dedicated to a single purpose, and it's still growing to the planned 24 satellite constellation consisting of 21 satellites and three on-orbit spares.. The Master Control Station (MCS), located at Falcon Air Force Base is responsible for the maintenance of the GPS satellites and their payload. The navigation payload of each satellite is regularly updated with orbital parameters, atomic frequency standard states, and almanac data for broadcast to the user community. This paper will briefly describe the Navstar system, the arrangement and organization of the MCS, and the Kalman Filter algorithms used by the MCS. The paper will go on to describe the ways in which the MCS manages those algorithms. Nominal performance as well as performance under anomalous conitions will be discussed. The improvement in orbital adjust modeling will be explained.

THE NAVSTAR SYSTEM

The GPS satellites operate at an altitude of approximately 20183 Km in a near circular orbit with a 12 hour semisynchronous orbit. Orbit inclination for the operational satellites is 55 degrees. Each satellite transmits two

L-Band signals. The L1 signal is a radio carrier frequency of 1575.42 MHz. The L1 signal is modulated by two pseudo random noise (PRN) codes known as the course acquisition (C/A) and precision (P) codes which are in phase quadrature with each other. The P code is a PRN stream of 10.23 Mbits per second compared to the C/A code's rate of 10.23 Kbits per second. The L2 carrier operates at a frequency of 1227.6 MHz and usually only contains the P code. Both the P and C/A PRN codes contain the modulated data representing the navigation message from the transmitting satellite. This navigation message is transferred at a rate of 50 bits per second. The navigation message contains the satellite's clock offsets from GPS time, the satellite's precise ephemeris, and course almanac information for the entire operational GPS constellation. Other parameters are included in the navigation message to indicate the health of the GPS satellite, give single frequency users ionospheric correction information, and provide Universal Time. Users can either receive the single C/A code, or use the C/A code to acquire the P codes on L1 and L2. All clocks in the Navstar System are synchronized to GPS time.

Once the user reads the navigation message from each of the visible tracking satellites, the user can synchronize his time to GPS time, calculate the apparent range to the satellite, and solve for position using the formula:

$$PR_i^c = \sqrt{(X_i - X_u)^2 + (Y_i - Y_u)^2 + (Z_i - Z_u)^2} + c\psi_u \qquad (1)$$

Where,

$(X_i, Y_i, Z_i)^T$ = Satellite Inertial Position

$(X_u, Y_u, Z_u)^T$ = User Inertial Position

PR_i^c = Ionospherically Corrected User Pseudorange Measurement From The i'th satellite

c = The Speed of Light

ψ_u = User Clock Offset from GPS Time

Since the satellite inertial positions at a given GPS time are derived from the navigation message and pseudorange measured from the PRN code time differences, the only unknowns are the user's inertial position and the user's clock actual offset from GPS time. Since their are four unknowns, four pseudorange measurements from four different satellites are required to find the user's inertial position and clock offset. Table I shows the specifications for GPS user accuracy compared with other navigation systems. Obviously for this system to work properly, knowledge of the satellite's ephemeris and clock offsets with respect to GPS time must be precise. The GPS Operational Control Segment (OCS) is charged with keeping the navigation message accurate and the spacecraft in good operating condition.

The Operational control segment consists of five L-Band Monitor Stations (MS), three S-Band Ground Antennas (with two additional antennas available on a part time basis), and the Master Control Station (MCS). The locations and coverage of these ground stations is shown in Figure I. The L-Band tracking data is transmitted from the monitor stations to the MCS. The MCS uses this information to generate new orbital elements and clock states which are transmitted through the ground antennas to the satellite. Information on the satellite's status is also gained from the ground antanna S-Band telemetry. This system is pictured in Figure II. The GPS MCS is the hub of all the activity in the command and control of the Navstar system.

THE MASTER CONTROL STATION MANNING

The GPS Master Control Station's operations center is staffed with seven members of Air Force Space Command's Second Satellite Control Squadron. This group of seven people comprise the basic space operations crew. There are five crews, each working for a period of six days followed by four idle days. The off days provide for crew rest, as well as training and standby days. These operations crews maintain the Navstar constellation's state of health and navigation performance around the clock, every day of the year.

There are currently six positions in the operations center filled by the seven crew members. The Ground Controller is responsible for the communication links between the MCS and each of the four ground antennas and five monitor stations. The Satellite Operations Officer is the position tasked with making contact with a given satellite from the MCS through a ground antenna to monitor a given vehicle's state of health and transmit any necessary commands. The Satellite Engineering Officer is responsible for ensuring that a spacecraft is in good operating condition, all commands

TABLE I: Comparison Of GPS Specifications To Other Navigation Systems. Accuracies Are Given For The Precise Positioning Service.

System	Position Accuracy (m)	Velocity Accuracy (m/sec)	Range of Operation	Comments
GPS	16 (SEP) 3-D	≥ 0.1 (RMS per axis) (Note 3)	Worldwide	Operational worldwide with 24-hour all-weather coverage. Specified position accuracy available to authorized users.
Loran-C (Note 1)	180 (CEP)	No velocity data	U.S. Coast, Continental U.S., Selected Overseas areas	Operational with localized coverage. Limited by skywave interference.
Omega (Note 1)	2,200 (CEP)	No velocity data	Worldwide	Operational worldwide with 24-hour coverage. System is subject to VLF propagation anomalies.
Std INS (Note 2)	1,500 max after 1st hour (CEP)	0.8 after 2 hrs (RMS per axis)	Worldwide	Operational worldwide with 24-hour all-weather coverage. Degraded performance in polar areas.
TACAN (Note 1)	400 (CEP)	No velocity data	Line of sight (present air routes)	Position accuracy is degraded mainly because of azimuth uncertainty which is typically on the order of ±1.0 degree.
Transit (Note 1)	200 (CEP)	No velocity data	Worldwide	The interval between position fixes is about 90 minutes. For use in slow moving vehicles. Better position fix accuracy is available with dual frequency measurements.

NOTE:
1. Federal Radionavigation Plan, December 1984
2. SNU-84-1 Specification for USAF Standard Form Fit and Function (F3) Medium Accuracy Inertial Navigation Set/Unit, October 1984
3. Dependent on integration concept and platform dynamics

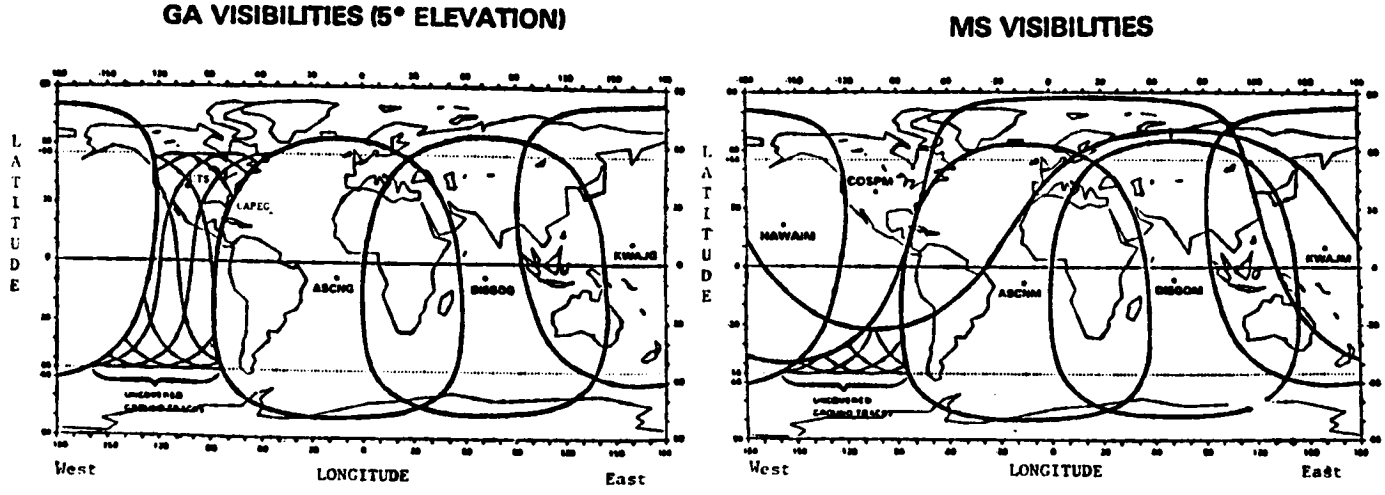

CTS - Colorado Springs Tracking Station
CAPEG - Cape Canaveral Ground Antenna
ASCNG - Ascension Island Ground Antenna
DIEGOG - Diego Garcia Ground Antenna
KWAJG - Kwajalein Atoll Ground Antenna

COSPM - Colorado Springs Monitor Station
ASCNM - Ascension Island Monitor Station
DIEGOM - Diego Garcia Monitor Station
KWAJM - Kwajalein Atoll Monitor Station
HAWAIM - Hawaii Monitor Station

NOTE: CTS and CAPEG give coverage over the Continental United States on a part-time basis.

FIGURE I: The GPS Ground Antenna and Monitor Station Locations and Their Respective Visibilities

sent to the spacecraft are valid, and to respond to any anomalous behavior.

The Satellite Analysis Officer monitors the L-Band tracking data from each of the monitor stations and verifies the navigation performance of the GPS constellation. The Deputy Commander takes care of all the bookkeeping and upchannel reporting of the crew's activities required in an Air Force operation. Finally, there's the Crew Commander who manages the entire crew and performs real-time rescheduling of the operations center's activities.

At the present time, there are two Satellite Operations Officers while every other position is filled by one crew member. The Ground Controller is at this time the only enlisted person on crew. Every other position is staffed by junior officers. The next ten years will probably see the Satellite Operations Officer positions grow to three slots and transition to enlisted personnel. The Deputy Commander position is also likely to be taken over by an enlisted person.

In addition to the operations crews, the Second Satellite Control Squadron supports these crews with several other sections. The Space Operations section directly supports the operations crews. The Scheduling Section produces a daily schedule of events which the crew follows. The Training and Standardization/Evaluation sections guarantee crew proficiency in their jobs. There's also an engineering support group which is broken down into sections responsible for the analysis of the spacecraft bus, navigation payload, ground system, and system database. Finally there is a section dedicated to interfacing with various users and a Command Section. All in all, there are approximately 100 people in the Second Satellite Control Squadron responsible for the operation of the GPS constellation.

It's the Satellite Analysis Officer crew position and the navigation payload section of the engineering analysis group which work with the contents of this paper. This group of people manages the Kalman Filter algorithms and results, guaranteeing the end product to the GPS positioning/timing users is usable, accurate, and within all published specifications.

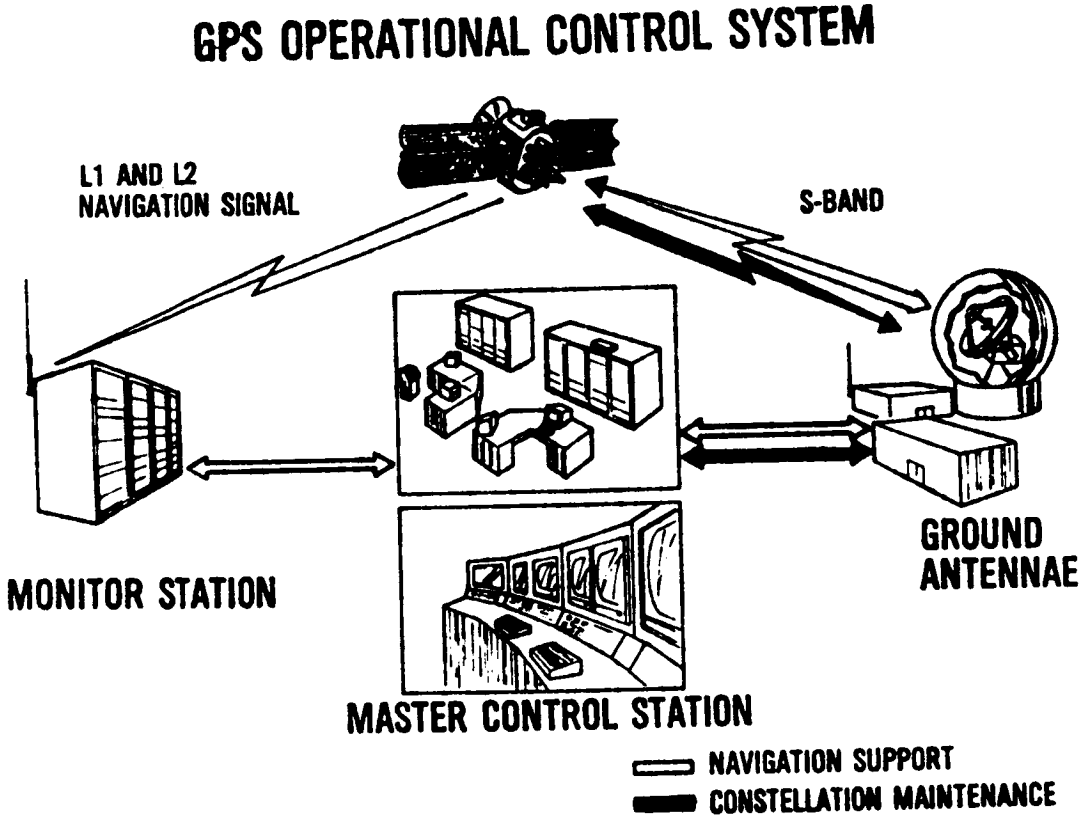

FIGURE II: The GPS Operational Control Segment. L-Band signals transmitted by each satellite are tracked by the Monitor Stations. Navigation Uploads, Telemetry, and Commands are routed through the Ground Antennas. The Master Control Station is the central processing location.

THE MCS KALMAN FILTER PROCESS

The two fundamental measurements made by the Navstar system are pseudorange (PR) and accumulated delta range (ADR). Pseudorange measures the distance between a satellite and a monitor station on the Earth by accounting for the total time between transmission and reception. This measurement is a "pseudo" range rather than a "true" range as a result of delays encountered on the signal's path to the Earth's surface. The equation used for pseudorange by the MCS is:

$$PR = c\left(t_{R_{MS}} - t_{T_{SV}}\right) \qquad (2)$$

Where,

- PR = Pseudorange Measurement
- c = Speed of Light
- $t_{R_{MS}}$ = Time Signal Received by Monitor Station
- $t_{T_{SV}}$ = Time Signal Transmitted By Satellite

The transmission time is represented by an integer number of z-counts where one z-count is equal to 1.5 seconds. The satellite and monitor station times are referenced to GPS time for synchronization.

Accumulated delta range (ADR) is a measurement of total phase accumulated between the transmision and reception of the carrier signal. Accumulated delta range is given by the expression:

$$ADR = \frac{c}{f}\left(\phi_{R_{MS}} - \phi_{T_{SV}}\right) \qquad (3)$$

Where,

- ADR = Accumulated Delta Range
- f = Carrier Frequency
- $\phi_{R_{MS}}$ = Monitor Station Phase Measurement
- $\phi_{T_{SV}}$ = Transmitted Satellite Phase

The only use for ADR's within the GPS control segment is to aid in the smoothing of pseudorange data. ADR's are available primarily for the GPS user community to calculate relative velocities.

The Master Control Station continuously tracks and collects pseudorange data from each satellite visible to the monitor stations. A pseudorange measurement is made every z-count on both the L1 and L2 signals received. Data processing occurs at fifteen minute intervals. As shown in Figure III, the MCS begins to store data at each fifteen minute point. Over each fifteen minute interval the satellite transmissions are checked for correct parity and C/A to P code Handover Word. Each measurement must also be within limits for signal/noise ratio, code and phase slips, code and carrier lock, and first and second difference tests. At the end of the fifteen minute interval there is a five minute waiting period. This waiting period is used to retrieve any data which may reside in a monitor station's data buffer due to short communications outages. After the five minute wait, the data which passed all editing critertia for raw pseudorange measurements during the fifteen minute interval are now ready for processing.

Each L1 and L2 measurement passing the editing criteria is now used to determine the ionospherically corrected pseudorange. The layers of the Earth's atmosphere approximately between 60 and 640 Km altitude constitute the ionosphere. The ionosphere can vary greatly over the surface of the Earth for such reasons as solar activity, the effects of man, and the variation between day and night. The ionosphere affects GPS by bending the transient carrier signals. Fortunately, the L-Band signal frequencies used bt the Navstar system exhibit the property that the index of refraction is proportional to the inverse square of the frequency. Since the two different carrier frequencies, L1 and L2, measure the same distance between the satellite and the monitor station, the proportionality constant can be determined independent of the actual ionospheric conditions or the elevation of the satellites. The proporionality constant is given by:

$$K_T = \frac{PR_1 - PR_2}{\left(\frac{1}{2f_1^2} - \frac{1}{2f_2^2}\right)} \tag{4}$$

where

PR_1 = Direct L1 pseudorange measurement
PR_2 = Direct L2 pseudorange measurement
f_1 = L1 carrier frequency = 1575.42 MHz
f_2 = L2 carrier frequency = 1227.60 MHz

Using the L1 measurement, the ionospheric time delay now becomes:

$$\Delta t_1 = \frac{K_T}{2cf_1^2} \tag{5}$$

So each pair of L1 and L2 pseudorange measurements received at every z-count is used to transform the raw pseudoranges to an ionospherically corrected pseudorange with the equation:

$$PR_I = c\left(t_{R_{MS}} - t_{T_{SV}} - \Delta t_i\right) \tag{6}$$

The ionospherically corrected pseudorange is the only calculation which occurs to the signal before filter processing. Other phenomenon which affect the signal, such as troposheric delay, relativity, and the free space delay are accounted for within the filtering system.

The ionospherically corrected pseudoranges are now smoothed over the 15 minute collection interval to reduce the measurement noise before Kalman Filter processing. A polynomial fit is made to the ionospherically corrected pseudoranges for each satellite-monitor station measurement pair. The smoothed pseudorange is determined directly from the polynomial and is set at the beginning of the fifteen minute interval.

The vector containing smoothed pseudoranges for each satellite-monitor station pair is defined as the observation vector. This observation vector will be processed by the MCS Kalman Filter to produce a state vector for each satellite and monitor station as shown in Figure IV. The state vector for each satellite includes its inertial position and velocity, a scaling parameter (K1) and an acceleration parameter (K2) for a solar pressure force model, and clock bias, drift, and drift rate. The monitor station state vector includes clock bias and drift, and tropospheric height.

To reduce the magnitude of the estimation problem, the MCS uses an independent partitioning scheme. Each partition is made of state vectors for up to six spacecraft and includes all monitor station states. This scheme reduces the processing load of the MCS, allows for isolation of satellites with poor performance, and gives the operator insight into the ground stations' states between partitions.

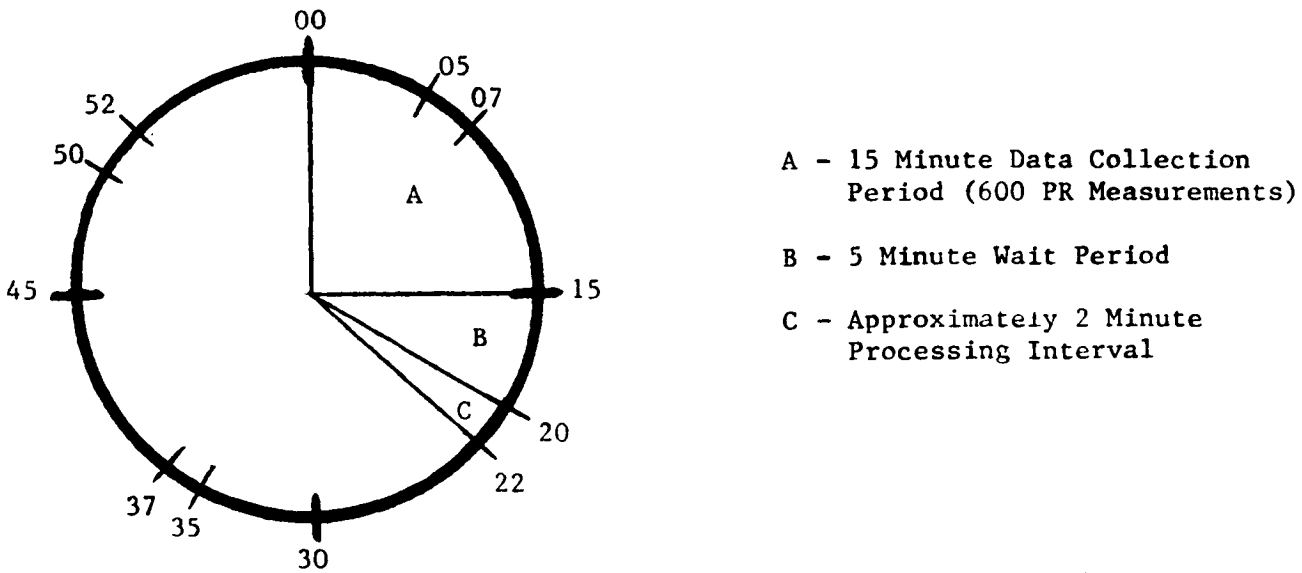

FIGURE III: Clock Representing The Time Intervals In Which The MCS Collects And Processes Pseudorange Data. The Cycle Shown Above Starts Every 15 Minutes.

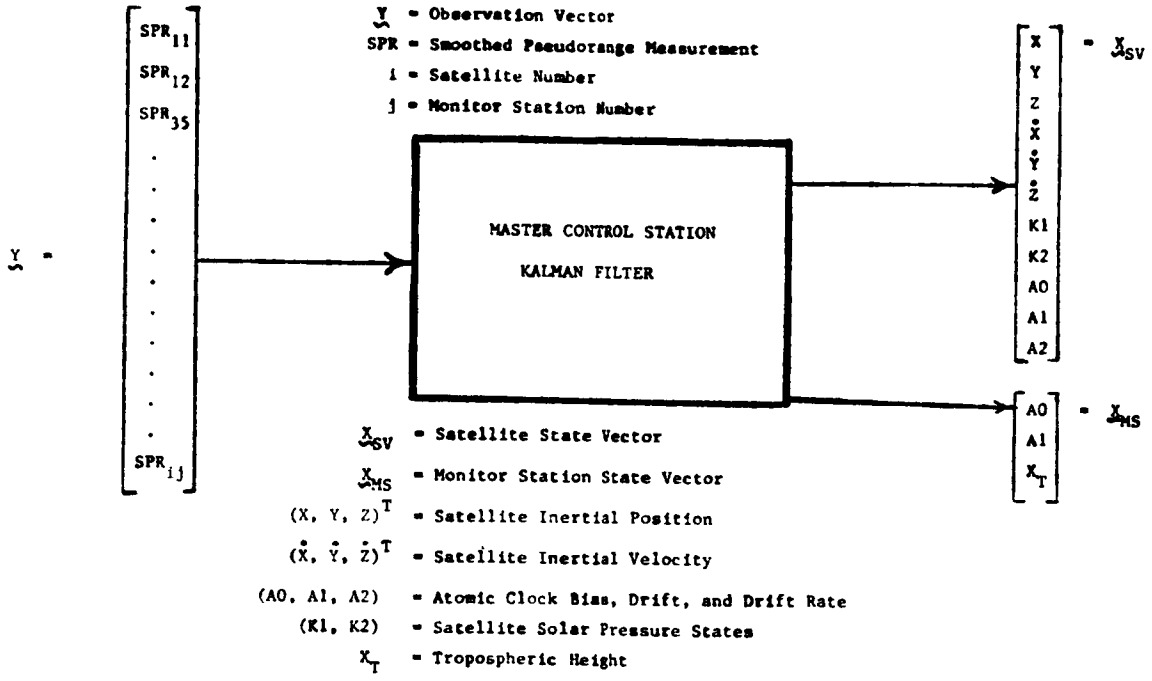

FIGURE IV: The MCS Kalman Filter Uses Smoothed Pseudoranges To Determine The Satellite And Monitor Station States Shown Above.

The purpose of the MCS Kalman Filter is to estimate the current states in a partition given the available measurements in the observation vector. In the MCS manifestation of the Kalman Filter, the current state process is linearized with respect to a reference system and then related to an epoch state residual process. The observation process is linearized about an apriori estimate of the state vector and likewise related to to the epoch state residual process. The formulation of the MCS Kalman Filter is described in the following paragraphs to give some context to the subsequent discussion of GPS Kalman Filter operations.

In the MCS implementation of the Kalman Filter, a predicted reference trajectory and a set of reference clock states exist. A simple relation is drawn between each state and the reference states at a specified time. For example, the current state residual is defined as the difference between the current state and the reference state at a current time:

$$\delta \underset{\sim}{x}_t = \underset{\sim}{x}_t - \underset{\sim}{x}_{ref(t)} \tag{7}$$

The epoch state residual is defined as the difference between the epoch state and the reference epoch state at the epoch time:

$$\delta \underset{\sim}{x}_0 = \underset{\sim}{x}_0 - \underset{\sim}{x}_{ref(0)} \tag{8}$$

The epoch states are mapped to the current states through a nonlinear state propagation model (F[...]) such that the reference state at current time can be found from the reference epoch state at epoch time:

$$\underset{\sim}{x}_{ref} = F[t, t_0, \underset{\sim}{x}_{ref(0)}] \tag{9}$$

The current state can be found from the epoch state and their associated times with:

$$\underset{\sim}{x}_t = F[t, t_0, \underset{\sim}{x}_0] \tag{10}$$

The relationship between the state residuals and their respective mapping functions is pictured in Figure V. Note that the reference state process shown in Equation 9 is a completely deterministic function.

For every state estimating partition, the state process is modelled in discrete time and given as:

$$\underset{\sim}{X}(T_{k+1}) = F[T_{k+1}, T_k, \underset{\sim}{X}(T_k)] + \underset{\sim}{w}(T_k) \tag{11}$$

Where, $\underset{\sim}{X}$ = State Vector

$\underset{\sim}{w}$ = State Process Noise

T_k = Time of Current Data Interval

T_{k+1} = Time of Next Data Interval

The state and state process noise vectors are dimensioned by the number of states in a partition. This current state process is linearized by substituting Equation 7, at the discrete time, into Equation 11 and then performing a first degree Taylor Series expansion on the current state residual term. With the substitution of Equation 9 at discrete time into the expansion, the current state residual is found to be:

$$\delta_{\underset{\sim}{X}(T_{k+1})} = \left.\frac{\partial F[T_{k+1}, T_k, \lambda]}{\partial \lambda}\right|_{\lambda = \underset{\sim}{X}_{ref}} \underset{\sim}{X}(T_k) + \underset{\sim}{w}(T_k) \tag{12}$$

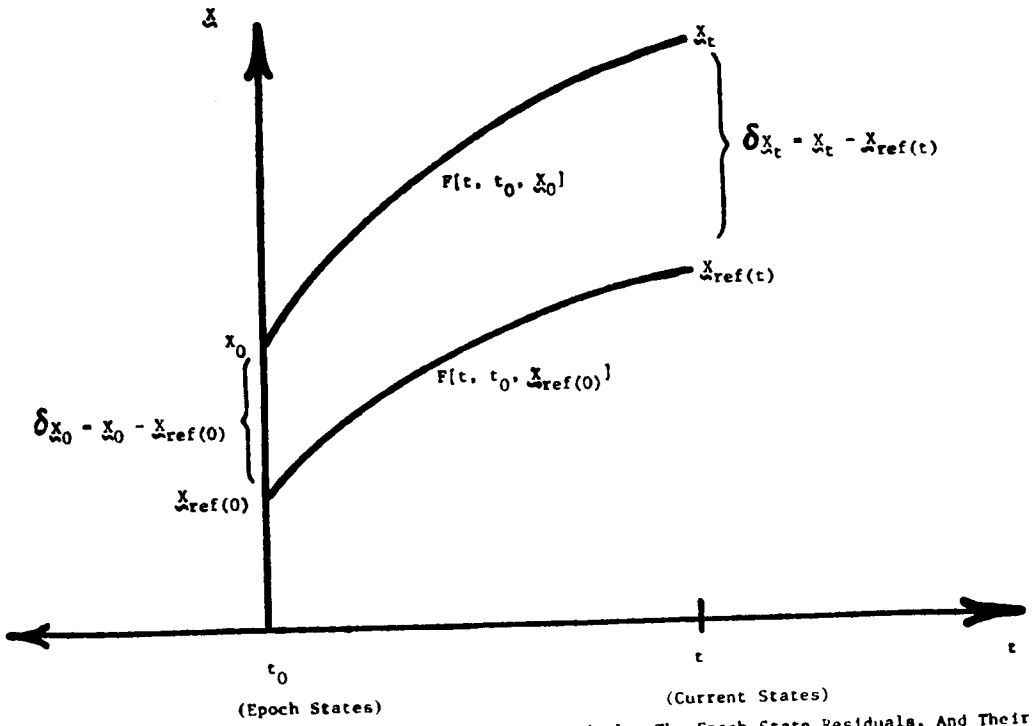

FIGURE V: Interrelationship Between The Current State Residuals, The Epoch State Residuals, And Their Mapping Functions.

By following the same logic, the current state residual is related to the epoch state residual by linearizing the mapping function with respect to the reference epoch state. Substituting Equation 8 into 10, performing a Taylor Series expansion on the epoch state residual term, and substituting Equation 7 results with the equation:

$$\delta_{\underset{\sim}{X}(T_k)} = \left.\frac{F[T_k, T_0, \lambda]}{\partial \lambda}\right|_{\underset{\sim}{X}_0(T_k)} \Bigg|_{\lambda=\underset{\sim}{X}_0} \tag{13}$$

If the two discrete time forms of Equation 13 are substituted back into Equation 12 and algebraically manipulated, the final result is the epoch state residual process used by the MCS:

$$\delta_{\underset{\sim}{X}_0(T_{k+1})} = \delta_{\underset{\sim}{X}_0(T_k)} + \left[\frac{\partial_{\underset{\sim}{X}_{ref}(T_{k+1})}}{\partial_{\underset{\sim}{X}_0}}\right]^{-1}_{\underset{\sim}{w}(T_k)} \tag{14}$$

The state process noise is assumed to be a white gaussian process with zero mean such that the expected values of the state process noise have the form:

$$E[\underset{\sim}{w}(T_k)] = 0 \qquad \text{and} \qquad E[\underset{\sim}{w}(T_k)\underset{\sim}{w}(T_L)] = Q(T_k)\,\delta_{kL} \tag{15}$$

δ_{kL} = Kronecker Delta

T_L = Any Other Data Interval

where Q represents the covariance matrix for each state. The covariances have a constant value defined in the MCS database, and are added at each Kalman Filter data interval.

The observation process is modelled in discrete time with the nonlinear equation:

$$\underset{\sim}{y}_t = h(\underset{\sim}{x}_t) + \underset{\sim}{v}_t \tag{16}$$

The observation vector and process noise are dimensioned by the total number of observations made by a partition. This equation relates the current state vector to the smoothed pseudoranges with the state transition matrix, h[] with the addition of measurement process noise. This observation process is linearized about an apriori state estimate and then expressed in terms of the epoch state residual. The resulting linearized equation is:

$$\underset{\sim}{y}_t = h(\underset{\sim}{\bar{x}}_t) + \left[H(\underset{\sim}{\bar{x}}_t)\right](\delta_{\underset{\sim}{X}_0} - \delta_{\underset{\sim}{\bar{x}}_0}) + \underset{\sim}{v}_t \tag{17}$$

where

$\left[\frac{\partial h}{\partial \underset{\sim}{\bar{x}}_t}\right]$ = The matrix containing the partial derivatives of the pseudorange measurement function with respect to each apriori state

$[\phi] = \frac{\partial \underset{\sim}{x}_{ref}}{\partial \underset{\sim}{x}_{ref(0)}}$ = Transition matrix

$$\left[H(\underset{\sim}{\bar{x}}_t)\right] = \left[\frac{\partial h}{\partial \underset{\sim}{\bar{x}}_t}\right][\phi]$$

As shown in Equation 2 the pseudorange measures the time delay between the time a monitor station received the given signal. This time difference can be broken down further to its components such that the observation model takes the form:

$$h(\underset{\sim}{X}(T_k)) = c\left[\Delta T_T(T_k) + \Delta T_{FS}(T_k, T_R) + \psi_{MS}(T_R) - \psi_{SV}(T_k) - \Delta T_r(T_k)\right] \quad (18)$$

Where,

ΔT_T = Tropospheric Delay
ΔT_{FS} = Free Space Delay
ΔT_r = Relativistic Delay
ψ_{MS} = Monitor Station Clock Offset
ψ_{SV} = Satellite Clock Offset
T_k = Signal Transmit Time = Data Interval Time
T_R = Signal Reception Time

The last three terms inside the brackets give the timing offsets between the monitor station and satellite clocks. The first two terms represent the propogation delay between the satellite and monitor station. Remember that the ionospheric delay has already been accounted for in the dual frequency corrections made before smoothing. The clock offsets are simply the time bias between either the satellite or monitor station clock and GPS time. The free space, tropospheric and relativistic delays will briefly be described.

The free space delay is experienced by a satellite's transmitted signal due to the physical propogation path length in vacuum. The free space delay is given as:

$$\Delta T_{FS}(T_k, T_R) = \frac{\left|R_{SV}(T_k) - R_{MS}(T_R)\right|}{c} \quad (19)$$

R_{SV} = Satellite Inertial Range

The monitor station reception time and the position vector for the monitor station phase center are found through an iterative process given the known transmit time.

The troposphere is the portion of the atmosphere which fills the volume between the Earth's surface to an altitude of about 12 kilometers. The major effect of the troposphere is to give an apparent increase in the signal path length. To help in the evaluation of tropospheric delay, three atmospheric parameters are measured at the monitor station recieving the signal. These parameters are atmospheric pressure, temperature, and dew point. Since different locations around the world can have widely varying conditions of the troposphere, the tropospheric height is modeled as a state variable in the estimation process of the Kalman filter. The tropospheric height is the actual altitude of the troposphere at the monitor station. The tropospheric delay is found with the equation:

$$\Delta T_T = \frac{1}{c}\left\{\frac{(0.02312)P_s\left[T_k - 4.11 + \frac{5(r_{mm} - r_{ma})}{148.98}\right]}{T_k\sqrt{1 - \left[\frac{r_{ma}\cos(\theta)}{r_{mm} + (1-l_c)(r_d - r_{mm})}\right]^2}} + \frac{(0.0746)E_0 X_T\left[1 + \frac{5(r_{mm} - r_{ma})}{X_T}\right]}{T_k^2\sqrt{1 - \left[\frac{r_{ma}\cos(\theta)}{r_{mm} + (1-l_c)X_T}\right]^2}}\right\} \quad (20)$$

P_s = Monitor station barometric pressure converted to Kilopascals
T_k = Monitor station measured temperature converted to the Kelvin scale
r_{mm} = The radial distance from the Earth's center to the meteorological sensors.
r_{ma} = The radial distance from the Earth's center to the monitor station antenna
r_d = Tropospheric dry radius
θ = Satellite elevation
X_T = Tropospheric height
E_0 = Estimate of the partial water vapor pressure

$$= (6.11)(10)^{\left[\frac{(7.5)T_d}{T_d + 237.3}\right]}$$

T_d = Dew point temperature
l_c = Assumed integration constant
= 0.95 when $\theta > 5.0°$

A satellite in orbit will experience the effect of special relativity due to its speed with respect to an observer on the Earth. To the ground observer, the satellite clock will appear to be behind. The same satellite will also feel the effect of general relativity because of the orbit's lower gravitational potential. To the same ground observer, the satellite clock will appear to be ahead. The effect of general relativity is greater so to compensate, the satellite's clock is built to run at 10.2999999545 MHz rather than the 10.23 MHz of the monitor station clocks. With the satellite in orbit the two clocks will appear to be synchronized.

Setting the satellite clock behind the monitor station clock would completely account for the relativistic effects if the satellite's orbit were perfectly circular. Since the satellite is never in a perfectly circular orbit, a periodic relativistic variance needs to be included with the equation:

$$\Delta t_r = \frac{-2e\sqrt{\mu a}}{c^2} \sin(E) \tag{21}$$

where

e = Orbit eccentricity
μ = Universal gravitational parameter.
a = Semi-major axis of orbit
c = The speed of light
E = Eccentric Anomaly From Kepler's Equation

At the end of each data collection interval, a Kalman Filter solution is used to find the current state vector with the linearized whitened epoch state process (Equation 14) and observation process (Equation 17). A time update occurs first. In the time update, the aposteriori state estimates from the previous data interval become the apriori state estimates for the current data interval. Process noise is added to the aposteriori covariance matrix to define the apriori covariance matrix for the current data interval. The equations dictating the time update are:

$$\delta\bar{\underline{x}}_0(T_{k+1}) = \delta\hat{\underline{x}}_0(T_k)$$

$$\bar{\underline{P}}_0(T_{k+1}) = \hat{\underline{P}}_0(T_k) + \left[B(T_k)\right] Q(T_k) \left[B(T_k)\right]^T \tag{22}$$

Where,

$\delta\bar{\underline{x}}_0(T_k)$ = Apriori estimate of epoch state residuals given past observations.

$\delta\hat{\underline{x}}_0(T_k)$ = Aposteriori estimate of epoch state residuals given past and current observations.

$\underline{P}_0(T_k)$ = Covariances of the epoch state residuals.

$Q(T_k)$ = Process Noise

$\left[B(T_k)\right] = \left[\Phi(T_{k+1},T_0)\right]^{-1}\left[G(T_k)\right]$ where: $\left[G(T_k)\right]$ is a wieghting matrix.

After the time update occurs, a Kalman Gain is calculated using the apriori states and expected covariance matrix:

$$\underline{K} = \bar{\underline{P}}_0 \left[H(\bar{\underline{x}}_t)\right]^T \left[\left[H(\bar{\underline{x}}_t)\right]^T \bar{\underline{P}}_0 \left[H(\bar{\underline{x}}_t)\right] + \left[I\right]\right]^{-1} \tag{23}$$

The aposteriori estimate of the epoch state residuals for the current data interval is now found from the equation:

$$\delta\hat{\underline{x}}_0 = \delta\bar{\underline{x}}_0 + \underline{K}\left[\underline{y}_t - h(\bar{\underline{x}}_t)\right] \tag{24}$$

$$\hat{\underline{P}}_0 = \bar{\underline{P}}_0 - \underline{K}\left[H(\bar{\underline{x}}_t)\right]\bar{\underline{P}}_0$$

Using Equations 8 and 10, the current states can be found from the epoch state residuals.

With the linearized epoch state process, if the current state deviation from the reference states becomes too large, the quality of the MCS Kalman Filter solution can degrade. To avoid this problem, the MCS updates reference trajectories every four weeks and whenever linearity limits are exceeded.

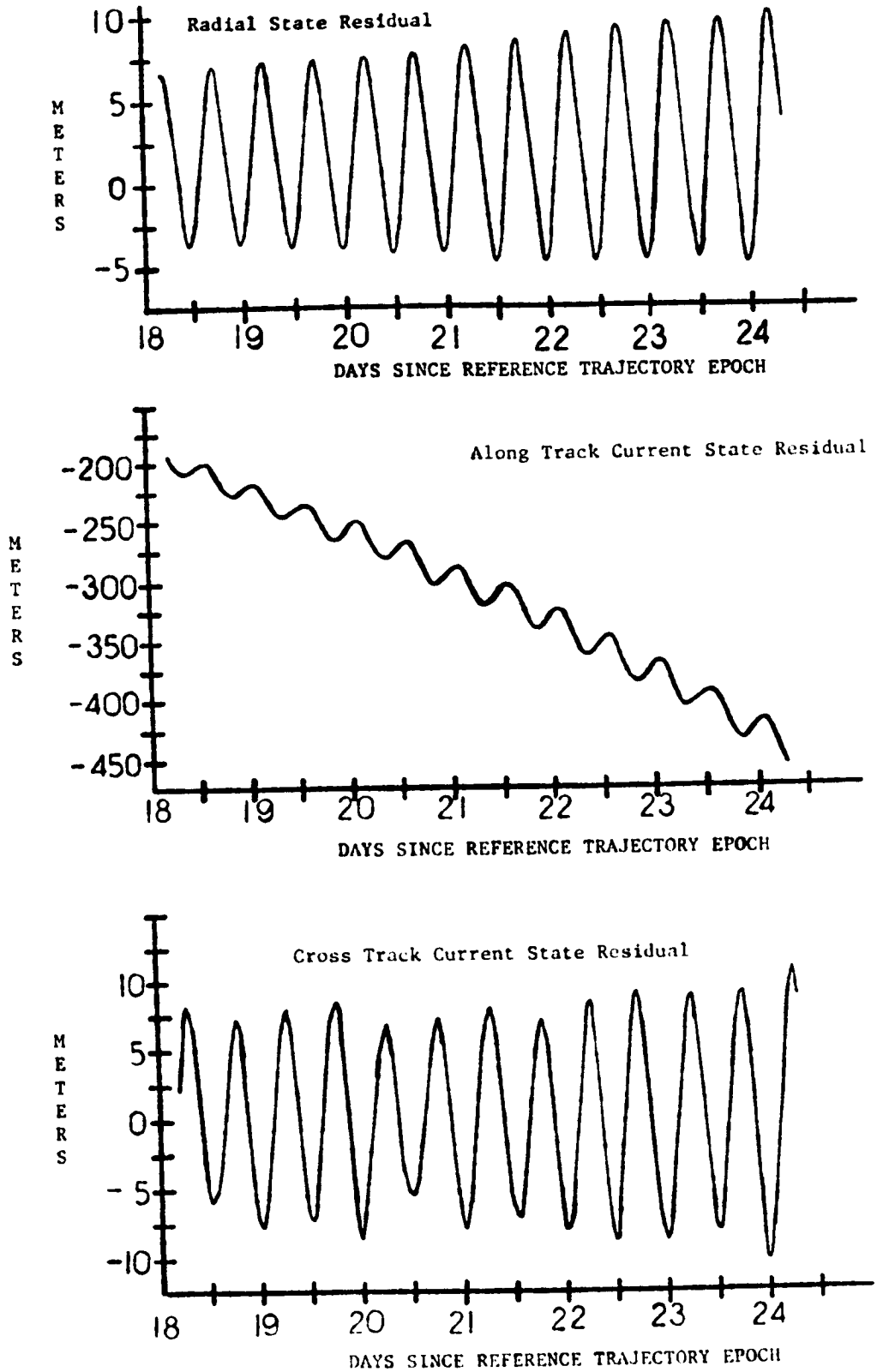

FIGURE VI-A: Typical Ephemeris State Performance. Inertial Position Offsets Have Been Transformed Into Body Radial, Along-Track, and Cross Track Deviations. The Offsets at Reference Epoch are Zero. On the 28th Day, The Current Reference Trajectory is Replaced with a New Reference Trajectory Based on the Current State Estimates at the New Epoch.

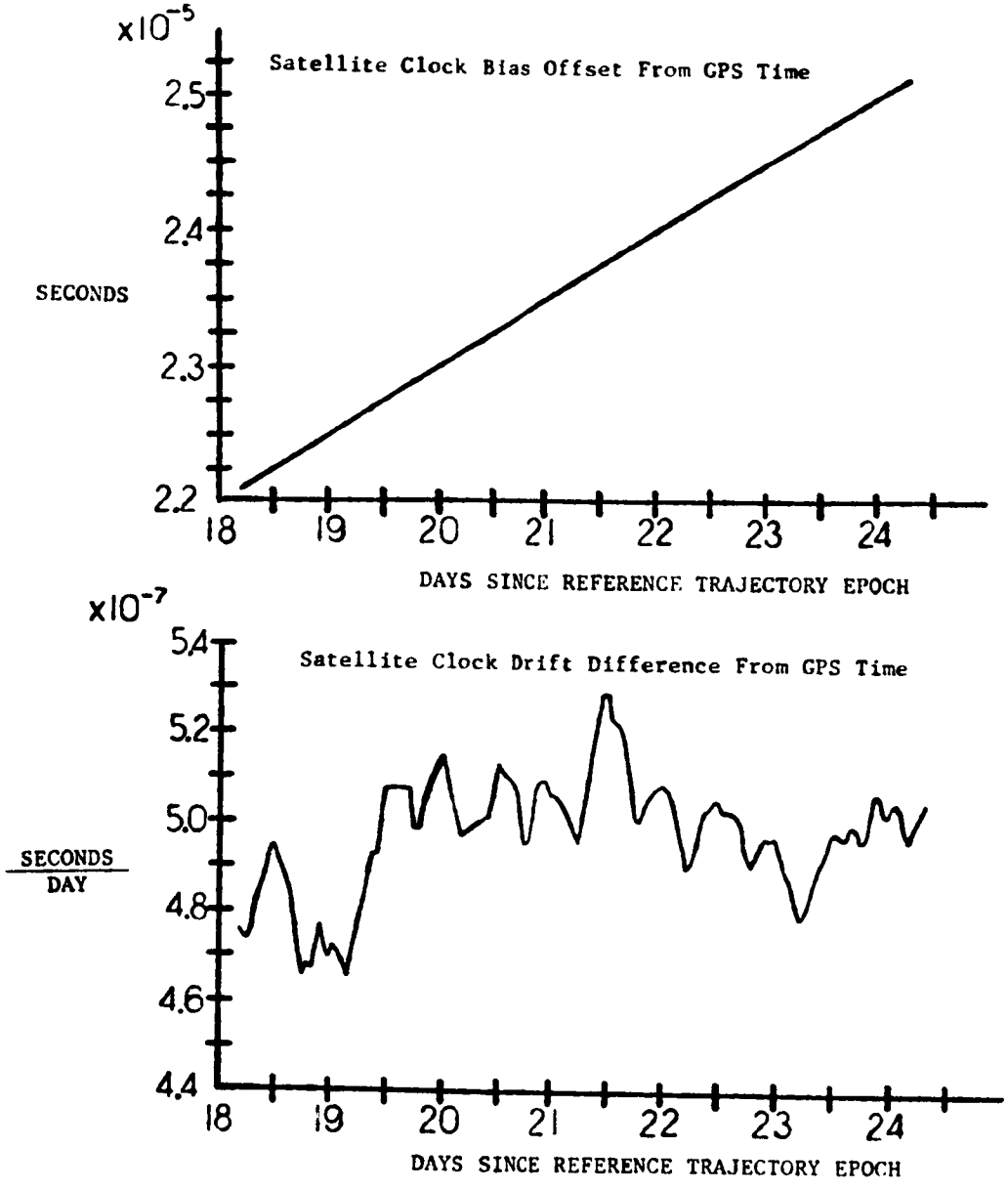

FIGURE VI-B: Satellite Cesium Atomic Clock State Bias and Drift Offsets From GPS Time. These Plots are also Typical of Normal Performance. The Reference States for Clocks in the GPS System are Determined from GPS Time. GPS Time is Derived from Either a Single Designated "Master Clock" or a Composition of All the Clocks in the GPS System. Note That There isn't any Apparent Influence on Clock States From Ephemeris States or Vice Versa.

MCS KALMAN FILTER OPERATIONS

Figure VI-A indicates the typical performance of current state residuals over a period of one week, approximately three weeks after a reference epoch. Aging of the reference trajectory states is evident over this period. The aging occurs because only major orbital perturbations are modeled by the Master Control Station. Figure VI-B shows typical cesium atomic clock performance compared to GPS time over the same period as the ephemeris states.

Epoch State Residuals, Current State Residuals, Epoch States, and Current States, as well as plots over a twenty-four hour period are all available for viewing to the Satellite Analysis Officer (SAO) at the end of each data interval. Though always available to the SAO, this information is usually only accessed when additional data on a given situation is needed.

The difference between the ionospherically corrected pseudorange and the pseudorange calculated from the apriori state estimates is called the pseudorange residual. The SAO observes the pseudorange residuals at the end of each data processing interval. The value of the pseudorange residual is usually below three meters. Values much above six meters are usually the first, and best indicator that there is a monitor station problem, satellite problem, or possibly a poor Kalman Filter model. If the pseudorange residual is above a dynamic limit based on the covariance matrix, the measurement obtained during the data interval is not used in the update of the Kalman Filter model.

When there are problems with the state estimates of a satellite or monitor station, the SAO has relatively few options to remedy the given situation. One option is to allow the process noise to add over time such that the measurement falls within limits some time in the future. This option generally isn't acceptable due to either the total time involved or the size of the rejected measurement. If the error can be attributed to a satellite or monitor station clock state, the SAO is capable of specifically modifying the clock state based on the observed pseudorange residuals. Another option left to the SAO is to change the value of the covariance matrix [P] in Equation 24. This action has been inappropriately called the "Q-Bump". It's possible to modify either monitor station, satellite, clock, ephemeris, or solar pressure state covariances. Any subset of these state covariances can be "Q-Bumped" at the same time. The value of the "Q-Bumped" covariances is prescribed in the MCS database and can vary with different situations. It's also possible to reinitialize the estimation problem, but this action is usually a drastic step. In some situations, various MCS database parameters can be changed which affect the behavior of the Kalman Filter algorithms.

There are two other tools used by the SAO. The first tool is the capability to mask the Kalman Filter. Masking prevents the update of the Kalman Filter state estimates with new data, thereby forcing only a time update to occur each data interval. The second tool is the capability, on a non-interference basis, to reprocess the Kalman Filter over a twenty four hour period with varying conditions. This reprocessing capability is quite powerful and chiefly responsible for the resolution of many problems.

The navigation data providing the GPS user community the precise ephemerides needed for accurate positioning are based on the Kalman Filter State estimates. When a navigation data upload is generated for transmission to a Navstar spacecraft, the satellite's ephemeris is predicted by using the aposteriori state estimates to differentially correct the reference trajectory. The clock states are predicted merely by propagating the aposteriori clock state estimates into the future. These ephemeris and clock state predictions are transmitted to the spacecraft with S-Band and, through the satellite, transmitted to the user community L-Band at the appropriate time.

The Master Control Station's insight into the quality of the upload prediction is performed with two statistical measures using the Kalman Filter state estimates. The first measure is the Estimated Range Deviation (ERD). The ERD is the difference between the aposteriori estimate of pseudorange and the pseudorange derived from the upload prediction for a particular vehicle. The ERD is calculated for a mathematically determined set of locations around the world and each GPS satellite visible to those locations. Normally ERD's grow over time indicating a slow degradation of the upload prediction. Figure VII shows this aging process. The need to upload each Navstar spacecraft with new navigation data on a daily basis is apparent in Figure VII to maintain the specified navigation performance. ERD's usually vary a little more than shown in Figure VII due to such aspects as monitor station visibility, timing of the upload creation, and clock movement. The second measure of performance is the Observed Range Deviation (ORD). The ORD is the difference the ionospherically corrected smoothed pseudorange and the aposteriori pseudorange determined by the navigation upload state prediction. An ORD is produced for each satellite visible to a monitor station. The ORD can be a good indicator of navigation performance. Should the ERD's and ORD's rise above a tolerance, set by the MCS as 10 Meters, a contingency navigation data upload will be accomplished to maintain user specified accuracy. Equations describing the Pseudorange residual, ERD, and ORD are given below:

$$
\begin{aligned}
PRR &= SPR_{ij} - PR(\tilde{\underset{\sim}{X}})_{ij} = \text{Pseudorange Residual} \\
ERD &= PR(\hat{\underset{\sim}{X}})_{ij} - PR(\underset{\sim}{X}_{\text{upload prediction}})_{ij} = \text{Estimated Range Deviation} \\
ORD &= SPR_{ij} - PR(\hat{\underset{\sim}{X}}_{\text{upload prediction}})_{ij} = \text{Observed Range Deviation}
\end{aligned}
\tag{25}
$$

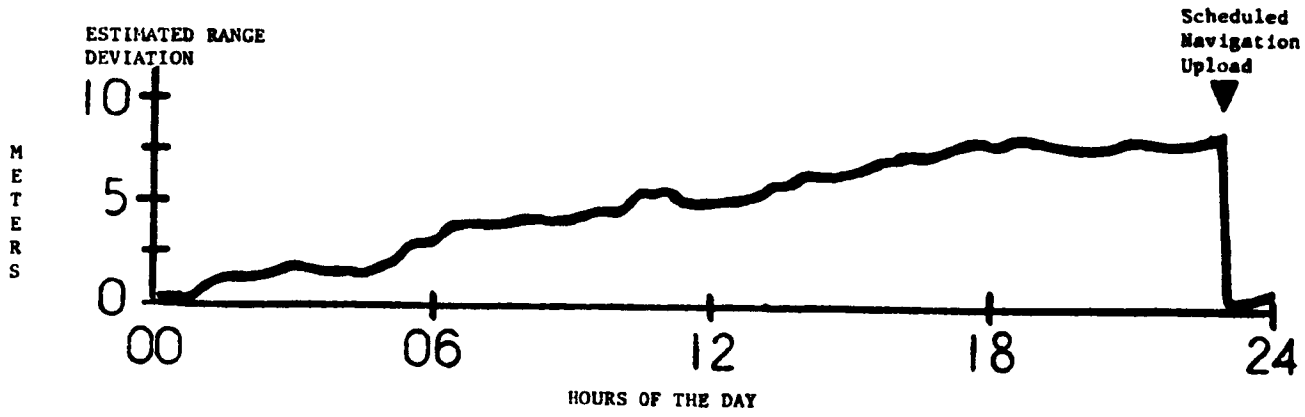

FIGURE VII: Typical Upload Prediction Performance as Reported by ERD's. Performance is Measured Against Range Based on Current State Estimates. Navigation Uploads Contain Ephemeris and Clock State Predictions Based on the Most Current State Estimates.

RESPONSE TO ANOMALOUS EVENTS

In January 1989, a Cesium atomic clock aboard Navstar vehicle number 11 failed. This failure necessitated a clock switch on board the spacecraft to a Rubidium atomic clock. A "Q-Bump" on the satellite's clock states was performed after the hardware failed. The Kalman Filter estimates had stabilized to new clock states in approximately six hours. This performance is shown in Figure VIII. The transient during this twelve hour period is readily observed. One month prior to the clock switch, the spacecraft bus section of the 2SCS engineering support group, predicted the cesium clock failure. As the time of the predicted failure approached the bad clock's performance was deteriorating. This deterioration is barely discernible in the clock drift plot shown in Figure VIII. Even with the deteriorated clock, performance of the satellite's navigation payload was maintained through a series of Kalman Filter clock state modifications and contingency navigation data uploads. On the fifth day of the year, maintaining performance through this means became impractical, so the satellite was set "Unhealthy" to the user community and the atomic clock was switched. At this time, the Kalman Filter was masked to prevent update of the satellite's clock and ephemeris states and the new Rubidium clock was allowed to "warm up". On the sixth day of the year, the clock state "Q-Bump" was performed. Clock performance was observed over the next several days and Navstar 11 was set back "Healthy". on the tenth day of the month.

Figure IX illustrates the impact of a satellite trajectory perturbance. In this case, Navstar 10 came out of a solar eclipse with an attitude error. This error was sensed by the spacecraft's Attitude and Velocity Control Subsystem (AVCS), and compensated with an attitude thruster firing. The impact on the trajectory in this instance was readily followed by the Kalman Filter State estimation process. In the situation shown in Figure IX, only a contingency upload was required to maintain navigation performance and a new reference trajectory was built approximately one week after the event to prevent linearity failures.

Satellite Vehicle thruster momentum dumps look very similar to Figure IX, but may be more severe. Normally the satellite will reduce reaction wheel momentum through variable setting magnets which torque the vehicle. Occasionally, momentum will saturate the satellite's reaction wheels at which time the vehicle's AVCS will command a thruster momentum dump. Sometimes this event may not be seen by the MCS due to visibility constraints. The momentum dump will manifest itself with growing ERD's and ORD's with respect to the ephemeris estimate and after twenty four hours, the pseudorange residuals will be rejected since the resulting states are above the calculated limits, indicating a mismodelling problem. In this situation, the Kalman Filter is reprocessed with an ephemeris covariance "Q-Bump" near the expected time of the thruster momentum dump. Usually only a contingency upload is needed to maintain navigation performance followed up later with a new reference trajectory based on the changed state estimates. If the pseudorange residuals, ERD's and ORD's are over tolerable limits the satellite is set "Unhealthy" to the user community.

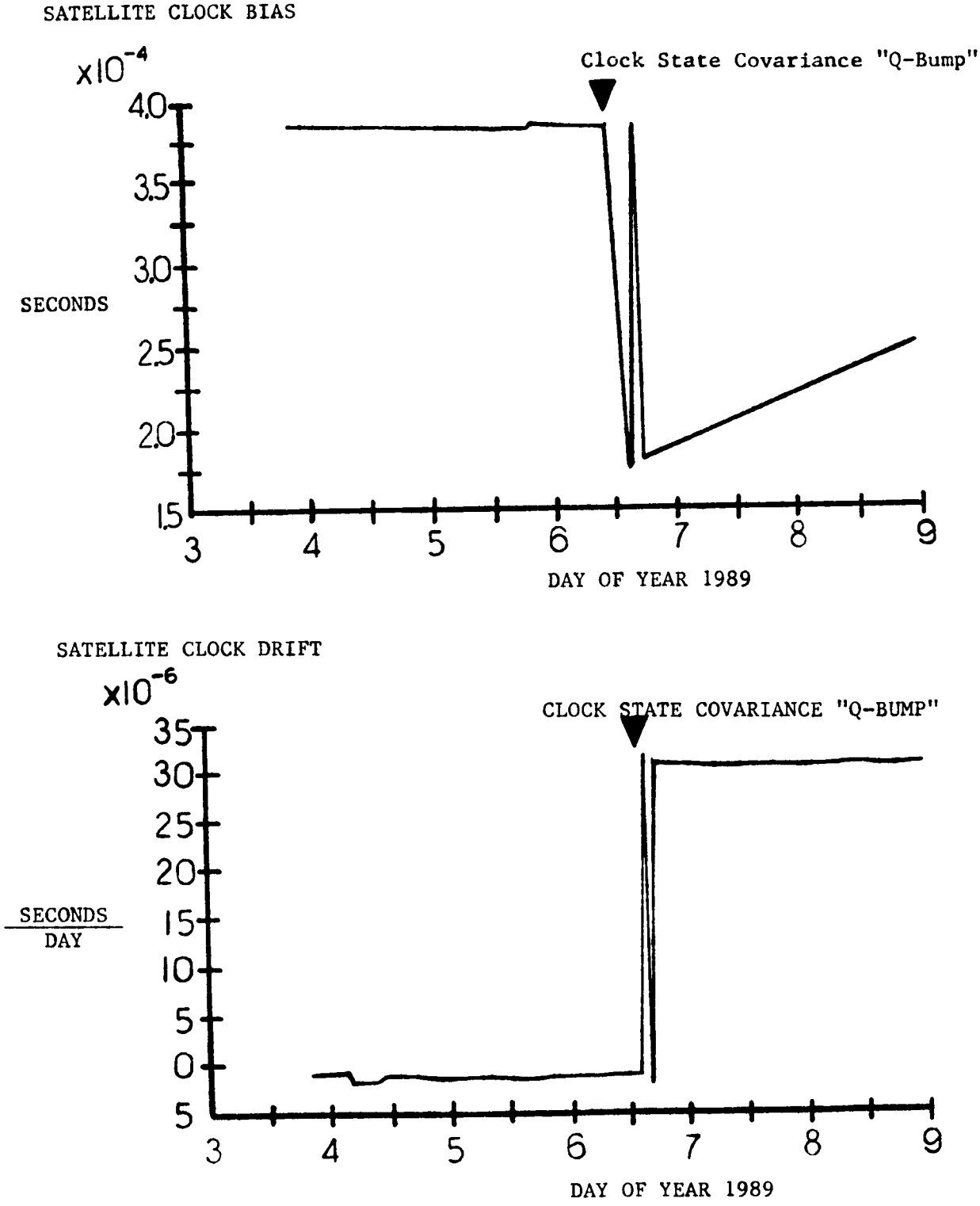

FIGURE VIII: The Satellite Clock State Reaction to a "Q-Bump" After a Clock Failure and Switch on NAVSTAR 11. The Determination of the New Clock States was Relatively Quick. Very Small Perturbations Affected the Ephemeris States. A Full Description of This Anomaly is in the Text.

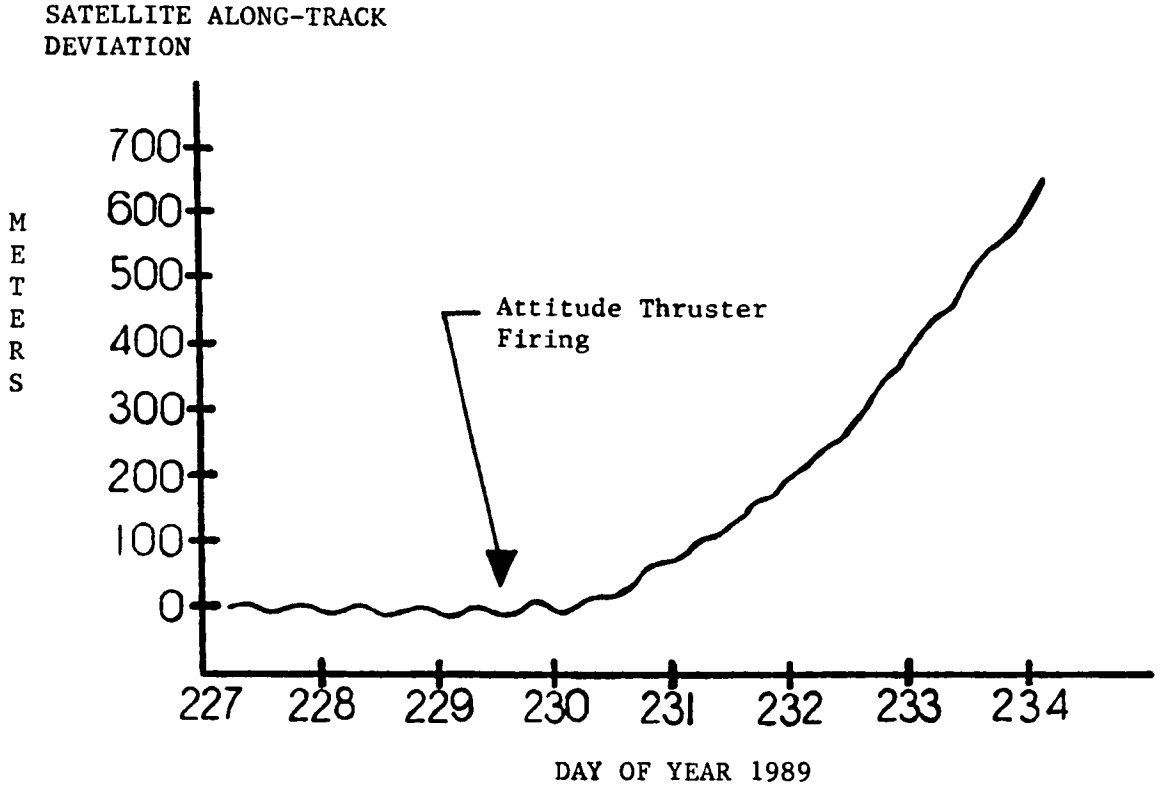

FIGURE IX: The Affect on Ephemeris State Estimates After an Attitude Thruster Firing on NAVSTAR 10. Satellite Thruster Momentum Dumps and Well-Modeled Delta-V Manuevers Show the Same Characteristics as this Plot. Radial and Cross-Track Deviations are not Shown for Brevity. There wasn't any Noticeable Clock State Perturbations due to this Ephemeris Change.

DELTA-V PLANNING AND MODELING IMPROVEMENTS

Prior to 1989, satellites undergoing Delta-V orbital maneuvers were usually set "Unhealthy" to the user community for a period of four days after the trajectory change. The engineers and the analysts in the 2 SCS didn't believe that this type of performance was acceptable. There were several efforts made to shorten the total "Unhealthy" time due to a Delta-V.

The first improvements were made in the area of Delta-V planning. The location of a GPS satellite is required to be at a specific longitude of ascending node with a tolerance of +/- 2 degrees. When a satellite originally approached this tolerance boundary, a station maintenance Delta-V was performed to return the satellite to its targeted geographic node. Since longitudinal acceleration always has a constant direction with respect to a specific geographic node, it was recognized that targeting for the far limit boundary would increase the time between station maintenance maneuvers. Figure X pictures the difference between these two targeting schemes. But there was one complication. Due to the configuration of the first generation GPS spacecraft, Delta-V's had to occur within specific beta-angle windows. This led into research directed at characterizing the performance of the 0.1 lb thrusters used for station maintenance maneuvers in GPS. Previous Delta-V planning tools modeled the thrust produced by the 0.1 lb rocket engine as an initial thrust followed by a linear decrease in force. Data from the manufacturer of the rocket engines showed a thrust build up to a peak followed by a decreasing force. The difference between these two thrust models is shown in Figure XI. Since small errors in the force model of a Delta-V can translate into large position errors several months down the road, a program was written incorporating this new thruster model. Aiming for maximum time between station keeping maneuvers with accurate beta-angle window placement reduced the number of Delta-V's and the total "Unhealthy" time due to station keeping.

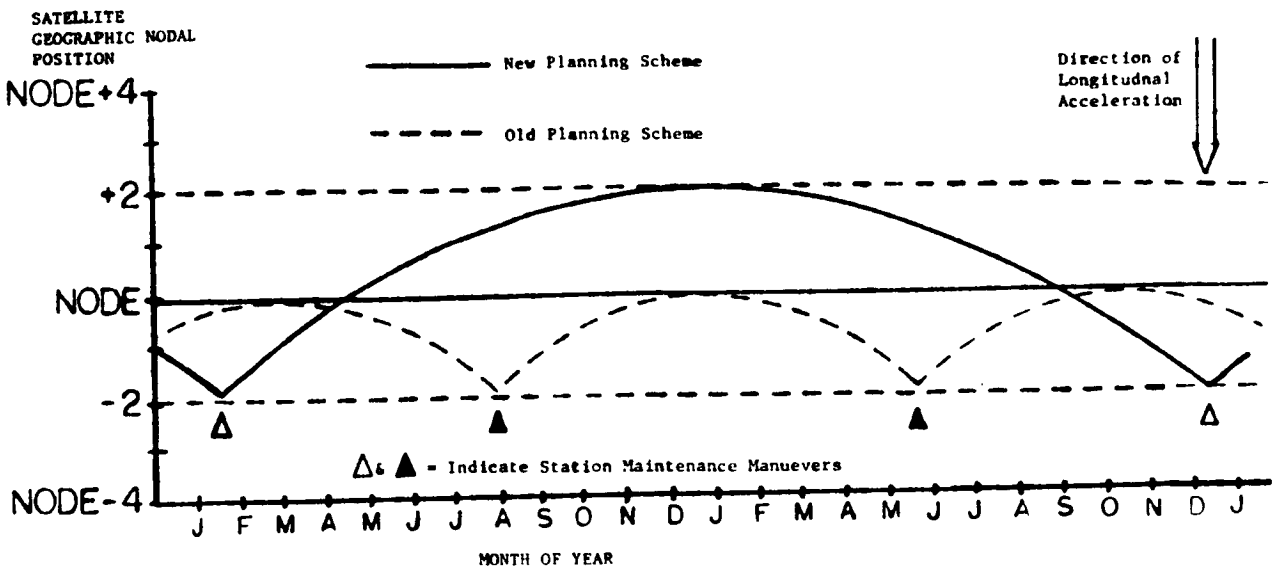

FIGURE X: Pictoral Representation Showing The Difference Between the Old and New Methods of Station Maintenance Manuever Planning. For The New Method To Work, Accurate Knowledge of Thruster Characteristics is Needed To Precisely Target a Beta-Angle Window.

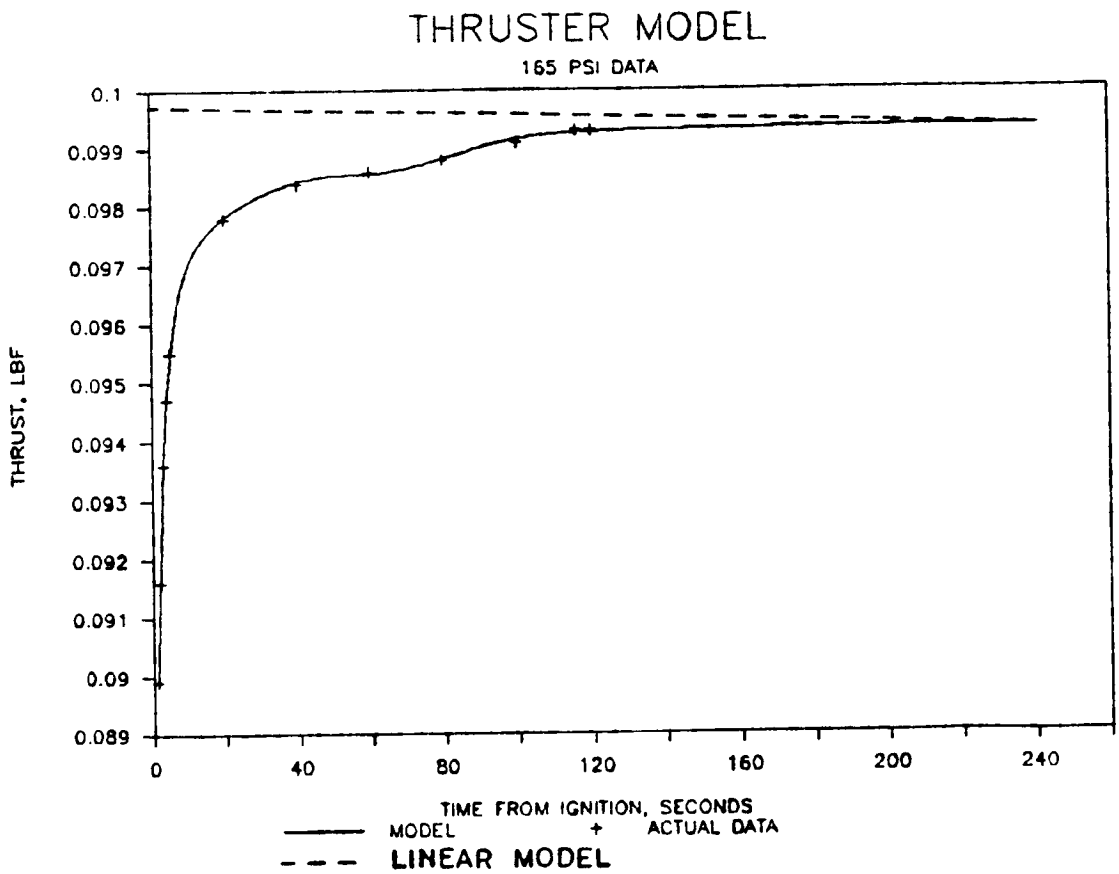

FIGURE XI: The Linear Thrust Model Compared to a Model Based On The Manufacturer's Test Data for The NAVSTAR Spacecraft 0.1 lb Hydrazine Thrusters. Incorporating The New Model Into The Planning Process for Station Maintenance Maneuvers has Improved Performance.

The MCS defines total Delta-V efficiency as the observed change in orbit semi-major axis compared to the expected change in the semi-major axis. The first generation, research and development (Block I), Navstar spacecraft tend to have Delta-V efficiencies of 92%. The second generation, operational (Block II) satellites generally have Delta-V efficiencies of 99%. Many factors can affect Delta-V efficiency including rocket exhaust body impingement, variable thruster efficiencies due to temperature, catalyst, engine misalignment differences, or attitude motion and attitude thruster firings. Figure XII shows a Block II satellite with major axis body reference frame. The 0.1 lb thrusters are located on a thruster pod as indicated in this figure. Block I satellites have a similar configuration. One major difference between the two types of vehicles is that the Block I spacecraft only have thrusters located along the Y body axis. Block II spacecraft have thrusters aligned along both the Y and X body axes. Given that the Y axis rocket engine exhaust impinges against the satellite body, and Block II Delta-V's are performed using the X body axis thrusters, the majority of the Block I Delta-V efficiency loss can probably be attributed to the thrust impingement. The Delta-V efficiency has been trended for each satellite and the MCS compensates for inefficiencies during the planning of a Delta-V. Unfortunately, Delta-V efficiency doesn't only vary from vehicle to vehicle, but between Delta-V's as well.

Delta-V maneuvers are modeled in the Kalman Filter's reference trajectory for the satellite undergoing the maneuver. Before 1989, an impulse model was used to account for the Delta-V in the reference trajectory. The impulse model instantaneously changes the reference trajectory at the midpoint time of the orbital maneuver. Though the impulse model was adequate for short duration maneuvers, Delta-V's of varying, and greater lengths than a few minutes were not well modeled. A thrust model was implemented which integrates the force of the rocket engines over the duration of the burn. This thrust model still uses the old linear force model mentioned above, but the prediction accuracy was still better than the impulse model. The thrust model had another advantage; the effects of attitude motion could be approximated with the available thruster misalignment inputs. When rocket engine characterization work began, a database of attitude motion during maneuvers also was started. This data could now be incorporated into the thrust model to better improve its prediction accuracy.

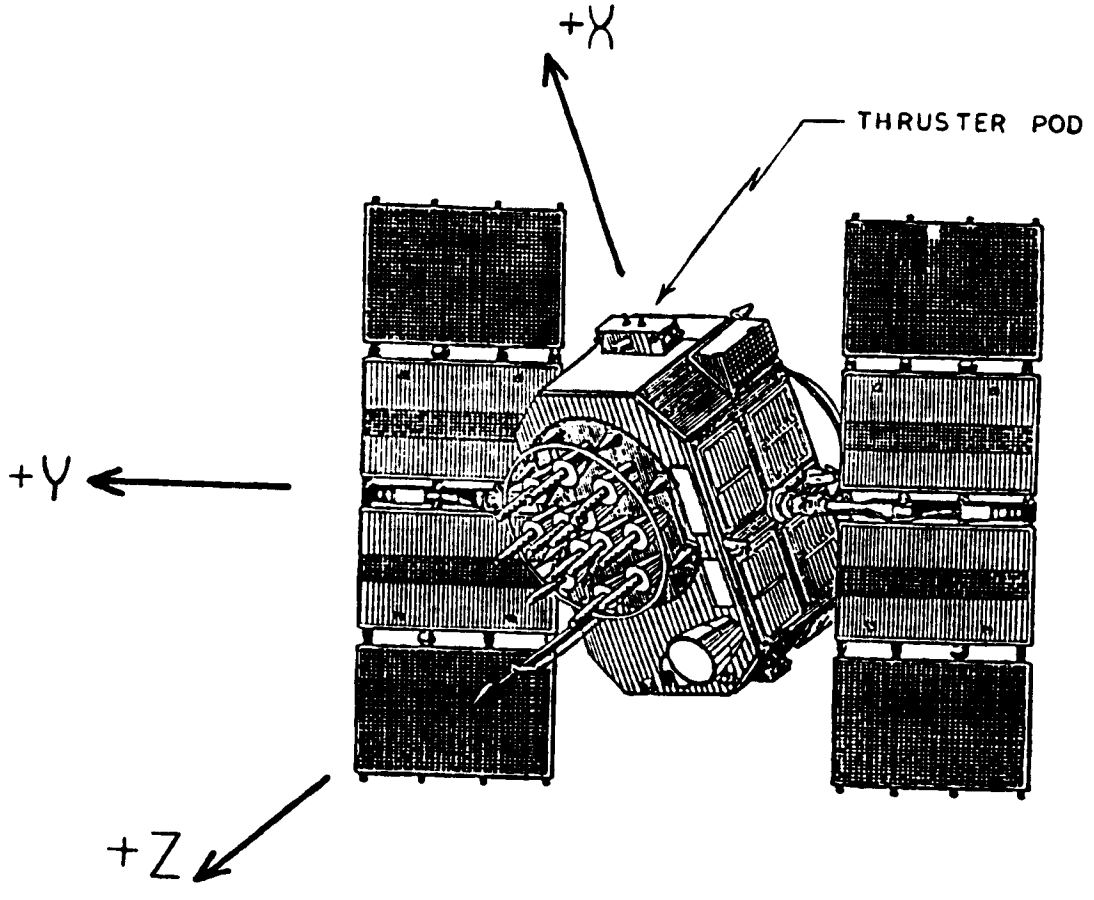

FIGURE XII: Picture of the Block II NAVSTAR Spacecraft with the Thruster Pod Indicated. On Block II Satellites, Station Maintenance Thrusters are Located Along Both The X and Y Axes, Though Usually Only The X Direction Thrusters are Used. Block I Satellites Only Have The Y Axis Thrusters.

Until very recently, immediately after a thruster firing, a "Q-Bump" on the satellite's ephemeris states was used to account for the errors in the Delta-V model. The parameters used in the covariance matrix for the "Q-Bump" were excessively large given the available thrust model. Work had begun on optimizing the values to set the covariance matrix after a Delta-V until it was discovered that the process noise expression in Equation 14 could be modified with values based on the Delta-V duration and expected error. Between the new thrust model, approximation of attitude errors, and the addition of maneuver process noise, large Delta-V's are beginning to look like the attitude thruster firing in Figure X. Before 1989, satellites were unavailable to the user community for up to four days after a maneuver. Today the same maneuver will cause under six hours of unavailability.

But improvements can still be made. An effort is under way to include the same rocket engine thrust curve pictured in Figure XI and used with maneuver planning in the reference trajectory thrust model. A rather simple relation is used currently to calculate the amount of process noise. Though this relation performs well, determination whether it's optimal needs to be made. In the near future, attempts to approximate the attitude thruster firing which occurs during a typical Delta-V will be made.

CONCLUSION AND RECOMMENDATIONS

Overall, The MCS Kalman Filter is quite robust. The bottom line is that highly accurate navigation data is routinely transmitted to a worldwide community of military and civilian users with minimal interruption in service. The online monitoring and control of the Kalman Filter is relatively simple. However, some improvements in the operation of the MCS Kalman Filter could be made. For example, many parameters which reside in the MCS database, such as the [P] matrix value for "Q-Bumps" or Delta-V process noise would yield more control if they were updatable on the online system. The aging of the reference trajectory would be less and ephemeris upload prediction would be better if more orbital perturbations were modeled. Better clock predictions should be possible.

The MCS should have a capability to monitor user accuracy that is independent of the Kalman Filter. The way ERD's and ORD's are calculated assumes that the Kalman Filter solution is truthful. It's easily possible for the MCS operators to see large ERD's and ORD's on a satellite which is a result of Kalman Filter corruption. Thanks to the MCS partitioning scheme this error can be caught rather quickly as the corruption starts to affect other states in the partition. Unfortunately it's still possible to be fooled and mistakenly upload satellites with corrupted data, therefore an independent check is needed.

For Delta-V's, it's apparent with the proper engineering data on a vehicle system and associated rocket engines, highly accurate trajectory predictions are possible. Though relatively late for the GPS system, satellite attitude motion and attitude thruster firings during a maneuver could have been accounted for real time with data from rate gyroscopes on board the satellite. This data could have been used in a specialized Kalman Filter routine designed for maneuvering spacecraft. To counter the variability in Delta-V efficiencies, it is highly recommended to have thrusters located on a satellite such that their thrust is directed outwards, minimizing any potential body impingement.

Finally, designers should be careful not to oversimplify the data available to the operator of systems incorporating a Kalman Filter, while not making the operation of the Filter overly complex. The full potential of a system should also be realized given the design constraints if at all possible. I believe the MCS Kalman Filter experience shows what operations personnel can pull off given the relative freedom to make improvements.

REFERENCES

1) Information on the general nature and history of the Global Positioning System can be found in:

"Global Positioning System" Volumes I, II, and III, Published by The Institute of Navigation, Washington DC., 1980.

2) Information on the design of the MCS Kalman Filter was obtained from:

"Computer Program Development Specification for the MCS Ephemeris/Clock Computer Program: Appendix A" USAF Contract F04701-80-C-0011, Specification Number CP-MCSEC-302C.

ACKNOWLEDGMENTS

Many thanks to Dr. Ming Chien, Dr. David Winfield, and Dr. John Berg for not only teaching me most of what I know about GPS, but also for playing nursemaid to myself and others through many of the activities mentioned in this paper.